NATIONAL UNIVERSITY OF SCIENCE AND TECHNOLOGY
POLITEHNICA BUCHAREST
Doctoral School of Aerospace Engineering

Decision No. 31 of 04.04.2024

SUMMARY OF THE DOCTORAL THESIS

THEORETICAL AND EXPERIMENTAL STUDIES FOR DETERMINATION OF ROLL DAMPING COEFFICIENT FOR CROSS CONFIGURATION

Author: Eng. Ionuț BUNESCU
Ph.D. Supervisor: Prof. Dr. Eng. Teodor-Viorel CHELARU

DOCTORAL COMMITTEE

President	Prof. Dr. Eng. Teodor Lucian GRIGORIE	from	UNSTPB
Ph.D. Supervisor	Prof. Dr. Eng. Teodor-Viorel CHELARU	from	UNSTPB
Reviewer	CS I Dr. Eng. Cătălin NAE	from	INCAS
Reviewer	CS II Dr. Eng. Sorin RADNEF	from	INCAS
Reviewer	Prof. Dr. Eng. Dragoș ISVORANU	from	UNSTPB

BUCHAREST 2024

Acknowledgement

The scientific development of this PhD thesis would not have been possible without the involvement, support and guidance of outstanding people, who, through their high competence and demonstrated dedication, played an essential role in my development as a researcher, inspiring me with the confidence to progress.

To Prof. Dr. Eng. Teodor-Viorel Chelaru,

Deep gratitude and sincere thanks for the trust, scientific guidance, patience and professionalism demonstrated, as well as for the full support and understanding provided during the entire doctoral period.

To CS I Dr. Eng. Mihai-Victor Pricop,

I wish to express my full gratitude and deep respect for the generous support, help, guidance, advice and ideas provided during the entire period of scientific research during my doctoral period. I would also like to express my sincere thanks for coordinating and agreeing to the use of data from the 671 PED project as project manager.

To Prof. Dr. Eng. Sterian Dănăilă and Prof. Dr. Eng. Laurențiu Moraru,

With great consideration and gratitude, sincere thanks to the guidance committee for the advice and ideas expressed during the entire process of developing the doctoral thesis.

To my colleagues Eng. Ciprian Chivu, with whom I designed the architecture of the device and chose its components, and who made the software and control and data acquisition programs of the device and operated the device during the tests, **CSIII Eng. Mihăiță-Gilbert Stoican,** with whose help I designed the device and completed its manufacture and assembly, and **CS Eng. Mihai-Vlăduț Hothazie,** with whose help I carried out the numerical study and interpreted the obtained results, special thanks for all the support, understanding and ideas offered during the realization of the doctoral thesis.

To National Institute for Aerospace Research "Elie Carafoli" - INCAS București.

Special thanks for the support and facilitation of the realization of the experimental campaign and for the agreement offered regarding the use of the results obtained from the 671 PED project in the framework of the doctoral thesis, to the general director, as well as to the colleagues who directly or indirectly helped in the realization of the device, experimental tests and numerical simulations. Also, sincere thanks for the financial support offered for the dissemination of the results in technical and scientific events, as well as through the publication of articles in specialized journals.

I would like to express my special thanks to my family, especially my wife, for their constant moral support, deep understanding and constant encouragement during the process of writing my PhD thesis.

The experimental and numerical results presented in this thesis were obtained within the HiSAEROD project (671 PED), financed by the Executive Agency for Higher Education, Research, Development and Innovation Funding (UEFISCDI).

CONTENTS

1. INTRODUCTION

1.1. GENERAL FOUNDATION OF THE THESIS

The aerodynamic damping coefficients are the critical parameters in the analysis of the dynamic behavior of aerospace vehicles, being determined as the ratio between the aerodynamic damping moments and the motion parameters, such as the oscillation frequency or the angular velocity of the model. These coefficients provide information on the dynamic tendency of a vehicle in a rotational motion.

In particular, the roll axis damping coefficient, which is defined as the ratio of the roll axis damping moment to the roll speed of the model. This coefficient is particularly relevant in the analysis of stability and control of aerospace vehicles, due to the fact that it reflects the tendency of the vehicle to suppress or mitigate unwanted rotations about the roll axis.

Damping moment refers to the aerodynamic moment developed by the vehicle while performing a rotational motion. This damping moment is of particular importance in influencing the dynamic behavior of the vehicle and in determining how it responds to changes in motion or disturbances in the environment.

Determination of aerodynamic damping coefficients is necessary for a complete characterization of an aerospace vehicle, study of its performance and stability, dynamic simulation and control system design [1].

1.2. THE OBJECTIVES OF THE THESIS

This thesis proposes the following objectives:

- Development of a new technique for identifying the aerodynamic damping coefficient on the roll axis by the forced rotation method;
- Calibration of the new method of measuring the aerodynamic roll moment within the forced rotation method with the standard Basic Finner Model (BFM) established for experimental tests in dynamic regime;
- Development of some methods of correction of the experimental data in relation to the error given by the mechanical damping and the geometric deviation of the model;
- Development of an experimental rig to allow the determination of the aerodynamic damping coefficient on the roll axis within the INCAS trisonic wind tunnel;
- The numerical study of the damping coefficient on the roll axis and the calibration of the calculation model with the experimental results;
- Aerodynamic characterization of the BFM from the point of view of the aerodynamic damping coefficient on the roll axis and the expansion of the current databases;
- Understanding the physics of the flow in the vicinity of the rotating model, capturing the interactions of the model with shock waves, flow detachment or induced vortices.

2. CURRENT STATE OF KNOWLEDGE IN THE FIELD

2.1. SHORT HISTORY

Due to the need to identify the aerodynamic damping coefficients on the roll axis, and not only, the large aerodynamic experimentation facilities have expanded their testing capabilities by developing dynamic test facilities, which is why starting with the work [14] more and more works, among which [15], [16] and [17], have been published presenting experimental results obtained in various facilities by various measurement techniques for the same model, namely the Basic Finner Model, a standard model for dynamic measurements. Experimental studies on the identification of the roll axis damping coefficient are still ongoing, as shown in [3], [18], and [19].

With the development of computational technique and numerical calculation models, studies have been carried out on the estimation of aerodynamic damping coefficients for various aerospace models due to their wide applicability and low cost compared to experimental testing. In the first papers dedicated to the numerical study of damping derivatives [20] and [21], the results obtained with the potential flow model of order I and II are presented. Later, the papers [22], [23] and [24] were published, presenting results obtained with flow models for fluids without viscosity, the Euler model. In recent years, high accuracy models such as RANS, LES or DES have been used to estimate aerodynamic damping coefficients as shown in papers [6], [7], [10], [25] and [26].

2.2. STATE OF THE ART

Currently, capabilities for dynamic blowing experiments exist only in a few research centers such as: NOL (Naval Ordnance Laboratory) [15], AEDC (Arnold Engineering Development Center) [16], NAL (National Aeronautical Laboratory) [17], ONERA (Office National d' Etudes et de Recherches Aerospatiales) [28], NASA LRC (Langley Research Center) [18], VTI (Vojnotehnicki Institut) [3] or INCAS (National Institute for Aerospace Research and Development "Elie Carafoli") [19].

On the other hand, the most representative numerical studies such as: [20], [21], [23], [24], [32], [10], [8] and [6] present new techniques and models of calculation, developed to increase the accuracy of the results and to reduce the need for high computational resources.

2.3. THEORETICAL FOUNDATIONS

The aerodynamic damping coefficient about the roll axis is the derivative of the rolling moment coefficient, C_l, with reduced rotation, $p^* = \frac{pd}{2V_\infty}$, providing information about the dynamic tendency of the model about the roll axis. Its calculation relation is as follows:

$$C_{l_p} = \frac{\partial C_l}{\partial \left(\frac{pd}{2V_\infty}\right)}, \tag{12}$$

where p is the rotational speed about the vehicle roll axis, d is a reference length, and V_∞ is the free stream velocity

For the evaluation of the aerodynamic damping coefficient around the roll axis, it is considered that the model has only one degree of freedom, the rotation around the roll axis, and due to the geometry considered for the evaluation, symmetry is considered both with respect to the xOy plane and the xOz plane, resulting thus the dynamic relationship for the roll axis motion analysis.

$$I_X\dot{p} = \frac{1}{2}\rho_\infty V_\infty^2 Ad\left[C_{l_0} + C_{l_p}\left(\frac{pd}{2V_\infty}\right) + C_{l_{\delta^*}}\delta^*\right] + M_f + M_m \tag{13}$$

where in the left member of the expression only the term $I_X\dot{p}$ remains due to the assumptions: $J_{XY} = J_{XZ} = J_{YX} = J_{YZ} = J_{ZX} = J_{ZY} = 0$, $I_{YY} = I_{ZZ}$ and $\dot{q} = \dot{r} = q = r = 0$, and in the right member the moment remains aerodynamically, the resultant moment of the frictional forces M_f and the motor moment M_m required to rotate the model. The aerodynamic term is composed of the roll moment, the roll axis damping moment and the control generated roll moment.

The relation (13) consists of the dynamic term, the aerodynamic terms, the friction term of the support system and the motor torque term. The dynamic term ($I_X\dot{p}$) presents the character of the movement of the model. It becomes zero when the model is in an equilibrium state, not rotating, or rotating at a constant speed. The aerodynamic terms $\left(C_{l_0} + C_{l_p}\left(\frac{pd}{2V_\infty}\right) + C_{l_{\delta^*}}\delta^*\right)$ are present while the analyzed model is in a fluid flow, otherwise these are null.

Based on relation (13) two particular cases of rotation of the analyzed model can be distinguished. A particular first motion is free rotation, in which case the model rotates under the influence of an aerodynamic moment or initial rotation, so that the motor moment is zero and the dynamic term is zero. The second particular movement is the forced rotation and consists in the fact that the model is forced to rotate by an external torque with a constant speed. In this case, the dynamic term is zero and the driving torque is zero. These two cases are presented in detail below.

2.4. CALCULATION MODELS

2.4.1. Forced rotation model

This model involves continuously rotating the model at constant speed under flow conditions, measuring the moment with which the model resists the rotation, this is the aerodynamic damping moment [1].

The assumptions of this method are the following:

- The roll velocity is constant: $p = ct,\ \dot{p} = 0$;
- The motor torque is not null: $M_m \neq 0$;
- The roll command is null: $\delta^* = 0$;

The characteristic relationship of the forced rotation method is:

$$M_m = \frac{1}{2}\rho_\infty V_\infty^2 Ad\left[C_{l_0} + C_{l_p}\left(\frac{pd}{2V_\infty}\right)\right] + M_f \tag{14}$$

In aerodynamic experiments, corrections are needed to cancel the parasitic roll moment and the friction moment. The two corrections are performed iteratively and independently as follows:

$$C_{l_p} = \frac{\left(M_m - M_f\right)_{CW} + \left(M_m - M_f\right)_{CCW}}{\frac{1}{2}\rho_\infty V_\infty Ad^2 \cdot p} \tag{19}$$

2.4.2. Free rotation model

The free spin model involves spinning the model at a certain speed and releasing it under flow conditions to rotate under the influence of aerodynamic loads, measuring the variation of the speed of the model with time, as shown in the paper [1].

The assumptions of this method are as follows:

- The roll velocity is not constant: $\dot{p} \neq 0$;
- The motor torque is null: $M_m = 0$;
- The roll command is null: $\delta^* = 0$;

The characteristic relationship of the free rotation method is:

$$I_X\dot{p} = M_{x_0} + M_{x_p}p + M_f \tag{20}$$

In the experimental testing, corrections are required to cancel the parasitic roll moment and the frictional moment. The two corrections are performed iteratively and independently as follows:

$$M_{x_p} = \frac{I_X}{2}\left\{\left[\left(\frac{\ln\frac{p_2}{p_1}}{t_2 - t_1}\right)_{WT} - \left(\frac{\ln\frac{p_2}{p_1}}{t_2 - t_1}\right)_{VC}\right]_{CW} + \left[\left(\frac{\ln\frac{p_2}{p_1}}{t_2 - t_1}\right)_{WT} - \left(\frac{\ln\frac{p_2}{p_1}}{t_2 - t_1}\right)_{VC}\right]_{CCW}\right\} \tag{27}$$

3. USED METHODOLOGIES

3.1. WORKING HYPOTHESES

3.1.1. Basic Finner Model

The model used in the study is the Basic Finner Model (BFM), also known as the Army - Navy Finner (ANF). This model is an established model for aerodynamic dynamic testing to obtain damping derivatives, being selected as the standard configuration for dynamic testing by STAI (Supersonic Tunnel Association, International) and AGARD (Advisory Group for Aerospace Research and Development).

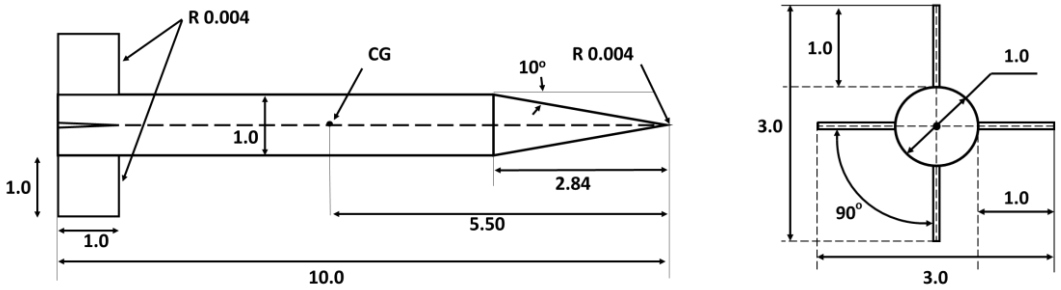

a) side view b) front view

Figure 5 Basic Finner Model

3.1.2. Testing matrix and reference dimensions

Considering the limitations of the experimental facility and the availability of experimental calibration results from the literature, the test matrix is as follows:

Table 1 – Testing Matrix

Mach [-]		0.4	0.8	0.95	1.2	1.6	2.0	2.5	3.0	3.5
p_0 [bar]		1.6	1.6	1.6	1.6	1.6	1.7	2.4	5.0	6.0
AoA [°]	Exp.	0-20	0-12	0	0	0	0	0-20	0	0
AoA [°]	CFD	0-50	-	0-50	-	0-50	-	0-50	-	0-50

3.2. EXPERIMENTAL TESTING

3.2.1. Experimental installation

The wind tunnel in which the aerodynamic experiments were carried out to identify the aerodynamic damping coefficient on the roll axis is the trisonic blower within INCAS.

3.2.2. Experimental techniques

In this study, two independent measurements will be made, using different experimental methods, namely: the free rotation method, a method developed in this

study whose results must be validated with reference results, and the forced rotation method, an integrated method for validation and consolidation reference database.

Considering the high costs of experimentation and the short burst times, the two considered measurements will be made within the same burst, initially using the forced rotation method, followed by the free rotation method as shown in Figure 9:

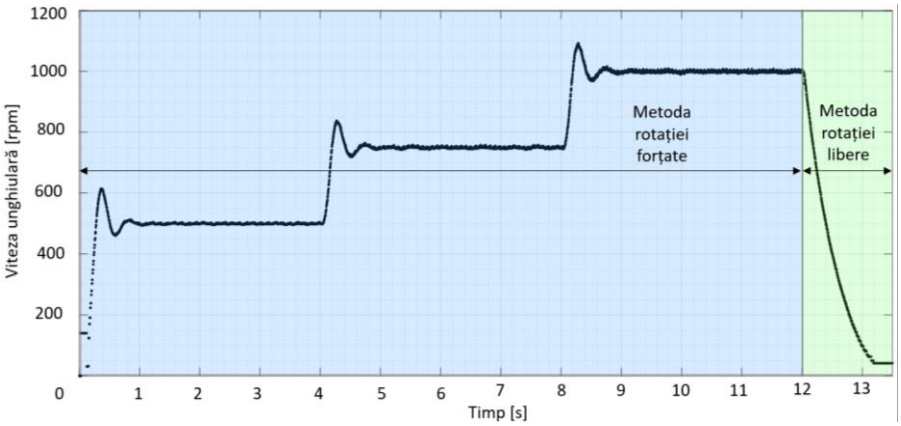

Figure 9 The sequence of methods used in experimentation

3.3. NUMERICAL ANALYSIS

3.3.1. The calculation models used

The mathematical model used for the numerical study is the RANS (Reynolds Averaged Navier-Stokes) model supplemented with the realizable k-ε turbulence model.

3.3.2. The calculation techniques used

In order to estimate the aerodynamic damping coefficients on the roll axis by numerical methods, regardless of the flow model used, computational techniques are needed to quantify the effect of movement (rotation around its own axis).

The predominantly used techniques are based on the division of the computing domain into different areas with interfaces between them that allow the exchange of information. The most used such solution techniques are: the Moving Reference Frame technique (MRFT) and the Sliding Mesh technique (SMT), these methods are briefly described in the following, being presented in detail in[43].

4. EXPERIMENTAL STUDY

4.1. OBJECTIVES OF THE EXPERIMENTAL STUDY

The experimental study presents the following specific objectives:

- Aerodynamic characterization with respect to roll axis damping for the standard Basic Finner dynamic test model at various Mach numbers and angles of attack in order to extend the current databases and increase their confidence;
- Development and validation of a method for measuring the damping moment on the roll axis to be used within the forced rotation technique in order to obtain the damping coefficient in a simpler and more accurate way;
- Development and validation of some methods of correction of experimental data obtained both from the point of view of strength and from the point of view of geometric deviation, with the aim of increasing the accuracy of the data and reducing the error band of the experimental data;
- The development of an experimental installation that allows the measurement of the damping moment on the roll axis both by the free rotation method and by the forced rotation method.

4.2. TESTING SYSTEM DESIGN

The test system, Roll Damping Rig, is the installation dedicated to determining the aerodynamic damping moment on the roll axis for aerospace models tested in the trisonic wind tunnel within INCAS. This system represents an extension of the blower's aerodynamic experimentation capability to the domain of dynamic regime testing, aiming to determine the aerodynamic derivatives on the roll axis for different flow regimes.

4.2.1. Presentation of the test system

The RDR test system is an extension of the aerodynamic testing capabilities in the trisonic blower of INCAS, which is why this system is designed so that it can be installed in the movable wall of the blower to perform the experiments at the desired angles of incidence. Figura 10 shows the longitudinal section through the plane of symmetry of the RDR test system:

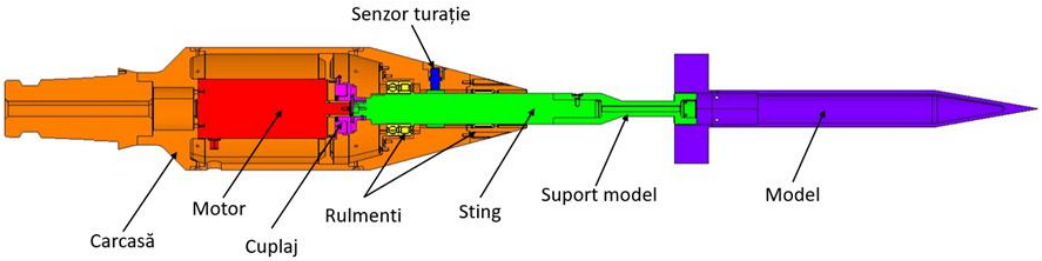

Figure 10 Longitudinal section through the RDR system

Figure 22, Figure 23 și Figure 24 show the RDR installation mounted in the experimental chamber of the blower.

Figure 22 Front view

Figure 23 Isometric view

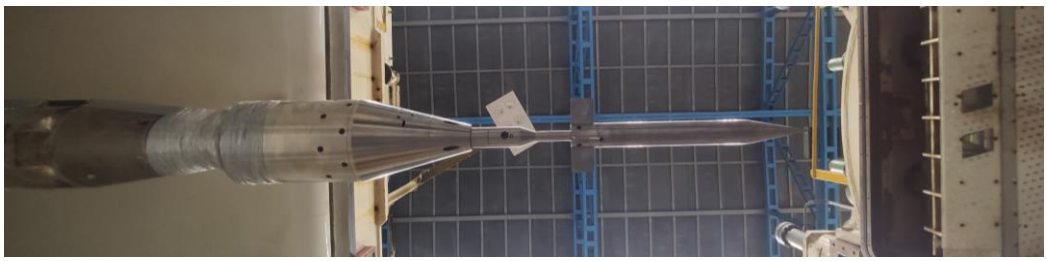

Figure 24 ventral view

4.2.2. Load estimation and structural analysis

4.2.2.1 Estimation of mass and aerodynamic loads

For the non-stationary starting regime there are no methods to evaluate the loads that occur, except for the normal shock wave method described in [45] and [46], which allows a robust estimation of the maximum loads that occur in the non-stationary valve opening regime until the flow is damped using the total pressure, Mach number and the projection of the model areas in the YoZ and XoY plane. This method uses the projection area of the model in the longitudinal plane of the model (A_N) and in the transverse plane of the model (A_F).

Critical aerodynamic demands are present in the supersonic regimes at the beginning of the experiments until the total pressure stabilizes. So the critical aerodynamic loads are presented in Table 3:

Table 3 – Unsteady supersonic aerodynamic demands

			Mach [-]	1.4	1.6	2.0	2.5	3	3.5	
	A_N [dm^2]	A_F [dm^2]	p0 [bar]	1.6	1.6	1.8	2.5	5.0	6.0	**F_A [N]**
BFM	0.049	0.003	**F_N [N]**	466	871	1565	2435	4550	3470	455
RDR	0.112	0.032	**F_N [N]**	998	1870	3349	5158	9534	7144	4853

4.5. THE RESULTS OBTAINED

4.5.1. The influence of corrections

4.5.1.1. Tare correction

This type of correction aims at extracting the contribution of mechanical effects (the effect of friction from the bearings) from the obtained results thus resulting in the aerodynamic contribution on the roll motion damping.

In order to identify the tare (mechanical damping of the system) a set of experiments is carried out with the RDR system without flow conditions.

Remarks:

From the presented results it can be seen that the effect of the force implies high deviations from the target result, especially at low speeds where the effects of friction in the bearings are significant in relation to the aerodynamic damping moment. It can also be observed that the variation of the corrected and uncorrected results with the speed has an asymptotic character to the right of the target value, the reason being due to the aerodynamic force.

Aerodynamic tare represents the effects of bearing friction due to aerodynamic loads, this is difficult to identify, the only option for aerodynamic tare correction is to make it negligible, rotating the model at very high speeds so that the damping moment is much larger compared with the frictional moments in the bearings due to aerodynamic loads. This practice of rotating the model at very high speeds is used in most of the experiments performed, including in the works: [15] și [29]. This effect is amplified in cases where the aerodynamic stresses increase, resulting in high stresses in the bearings, which induces an increase in friction in them, as observed in the transonic regime in Figure 43 or at high incidences in Figure 42 or Figure 46.

Another important aspect that can be observed from the presented cases is the similarity of the results obtained by the two methods: the forced rotation method (MRF) and the free rotation method (MRL). Although obtained independently, the values of the damping coefficient on the roll axis are very close, which implies an increase in the confidence of both methods developed in this paper (MRF) and the data itself.

As a general conclusion on the tare correction, it can be stated that this is an important correction, which provides a high accuracy of the results especially at low angular speeds where the damping moment is comparable to the friction moment.

4.5.1.2. Corrections with geometric deviation

This type of correction aims to extract the contribution of the parasitic aerodynamic moment due to the geometric deviation from the obtained results, thus resulting in the pure aerodynamic contribution to the damping of the roll motion.

In order to perform the correction with the geometric deviation, a set of wind tunnel experiments with the title "Correction" is carried out. These experiments are necessary to demonstrate a simpler correction method, which consider the slope of the points, instead of the ratio of the aerodynamic damping moment to the speed, presented in [1].

Remarks:

For cases of zero incidence, it is clearly observed that the raw data (both those obtained with MRF and those obtained with MRL) are positioned symmetrically with respect to the corrected data represented by a straight line passing through the origin of the system. The intersection of the regression lines built on the uncorrected results, with the oY axis, represents the coefficient of the aerodynamic moment resulting from the geometric deviation of the model, which is almost equal for the two directions of rotation, CW and CCW, respectively. Moreover, the intersection of the regression lines built on the uncorrected results, with the oX-axis, represents the value of the model angular velocity when the aerodynamic moment resulting from the geometry deviation is equal to the damping aerodynamic moment, without the contribution of another external moment. This parasitic speed is almost equal for the two directions of rotation.

Furthermore, it can be seen that the regression lines constructed on the uncorrected results have similar slopes both to each other and to the regression line of the corrected data, thus it can be admitted that the model does not necessarily need to be rotated both ways to determine the aerodynamic damping coefficient on the roll axis, but only one direction of rotation and a few points which provide their slope.

As a general conclusion on the correction with the geometric deviation, it can be admitted that this correction has a particular importance on the value of the roll moment coefficient, but for the damping coefficient on the roll axis, the correction method does not change much the value of the results.

4.5.2. Angular velocity variation in time

For a more detailed understanding of the aerodynamic damping phenomenon, the variation of speed with time when the model is allowed to rotate freely in flow conditions is presented below. The starting speed is the maximum speed used (i.e. 1000 rpm) and the rotation directions are both CW and CCW in order to observe the effects of the rotation direction on aerodynamic damping.

The cases presented in this section are the Mach 0.4 (0° and 20° AoA), Mach 0.95 (0° AoA), Mach 1.6 (0° AoA), and Mach 2.5 (0° and 20° AoA) cases. Within these analyzed cases, the useful calculation windows, the parasitic speed and the characteristics of the speed variation curves over time will be identified.

Remarks:

From the graphs shown, it can be seen that there are differences in variation between the curves determined by rotating the CW direction and those determined by rotating the CCW direction. Corroborating this information with the information in the section *4.5.1.2. Corrections with geometric deviation* it can be seen that the aerodynamic moments due to the geometric deviation generate these variation differences between the speed-time variation curves. Thus, for large parasitic moments, the variation differences are significant, and for small parasitic moments, the variation differences are insignificant.

Based on the influence of the parasitic moments, it is observed that for large parasitic moments, the parasitic speeds are also high, and for small parasitic moments, the parasitic speeds are low. So the variation differences between CW and CCW result

from the fact that the data determined by rotating CW first reaches 0 rpm, then the parasitic speed of the opposite direction (although on the graph they are shown in absolute terms), and the data determined by rotating CCW tends directly to idle speed (in the same direction) without passing through 0 rpm. Thus, due to the low parasitic speed present in certain cases, the trends of the variation curves are close.

4.5.3. Variation of damping moment with angular velocity

Figure 60 shows the variation of the damping coefficient on the roll axis with the angular velocity ($C_{lp}(n)$) considering the previous cases. From this figure it can be seen that although the data have a derivative character, they are consistent and precisely positioned with respect to the calibration lines. It can be distinguished that the data obtained with the MRF are positioned on the calibration line, while the data obtained with the MRL are positioned in its vicinity showing a slightly oscillating character, especially at the Mach 1.6 regime.

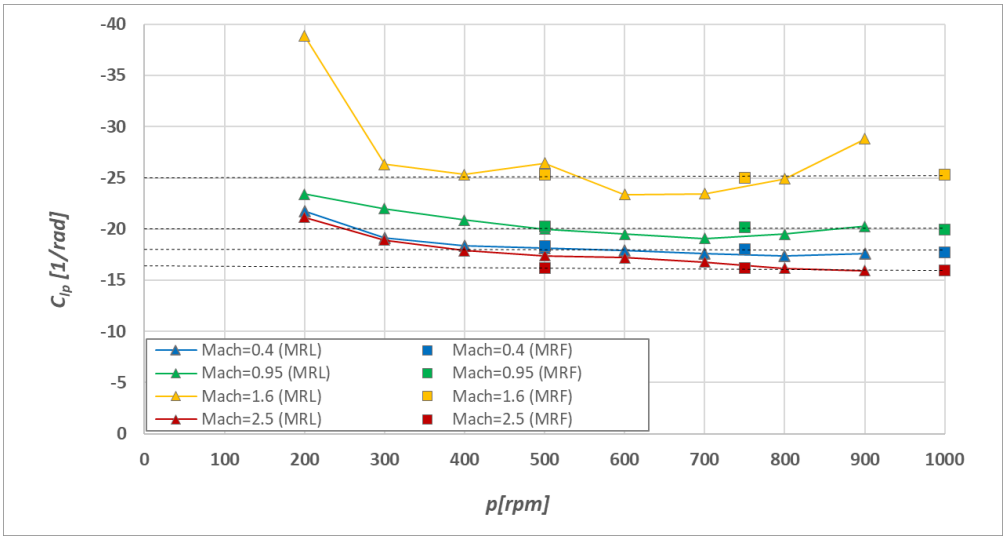

Figure 60 Variation of the damping derivative coefficient C_{lp} with speed

It can be seen that at revolutions below 500rpm, the values of the damping coefficient on the roll axis obtained by MRL deviate from the reference line, the reason being the effect of aerodynamic tare which becomes significant at low angular speeds. However, considering the values at high speeds, they show high accuracy, both in terms of MRF and MRL.

Remarks:

The results obtained show a very good precision, validating the methodologies used for data identification and correction. Thus, it can be stated that the aerodynamic damping phenomenon was captured by both the free rotation method and the proposed forced rotation method.

In addition, the effect of aerodynamic tare was observed, which at low revolutions induces an overestimation of the damping coefficient on the roll axis, a fact that can be avoided by considering high angular velocities, so that it becomes negligible.

4.5.4. Variation of damping coefficient with Mach number

In order to calibrate the device and verify the methods applied to obtain the experimental data, the variation of the damping coefficient on the roll axis with the Mach number is presented below, with reference data from NOL [15], BRL [14] and NAL [17] as can be seen from Figure 61.

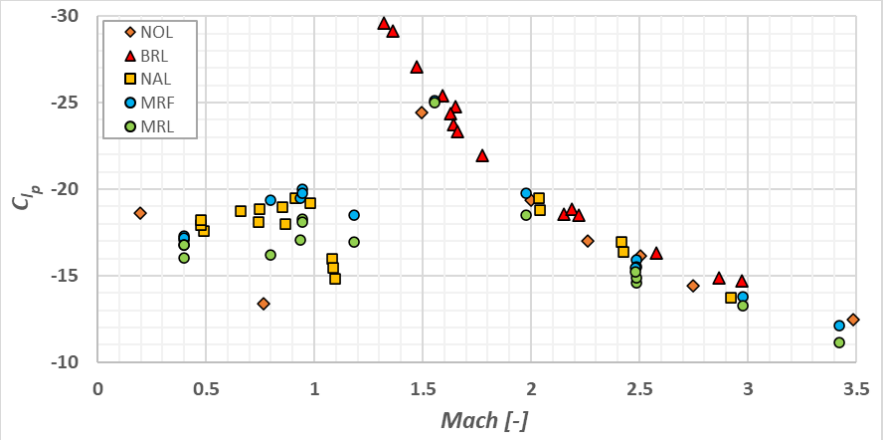

Figure 61 Variation of C_{lp} with Mach number

Figure 61 shows that the obtained results (MRF and MRL) are consistent with the reference results, the differences being minor and present only in the subsonic and transonic regimes.

4.5.5. The variation of the damping coefficient with incidence

This variation is present in only two sources, namely NAVORD [15] and AEDC [16], which are also used in this case to verify the obtained data. The considered Mach regimes are Mach 2.5, where reference data are available in both [15] and [16], and respectively Mach 0.4 being the minimum Mach number that can be obtained in the trisonic wind tunnel of INCAS, the reference data being considered for Mach 0.22 in [15].

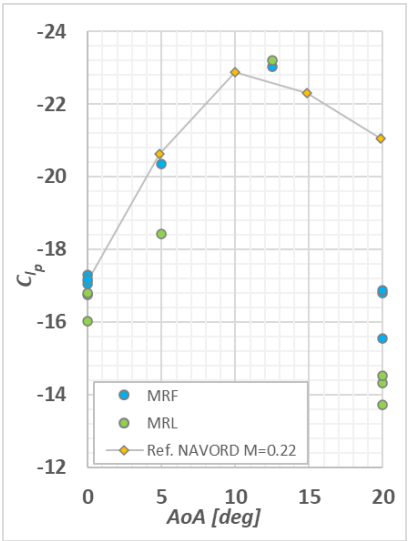

Figure 62 Variation of C_{lp} with incidence at Mach 0.4

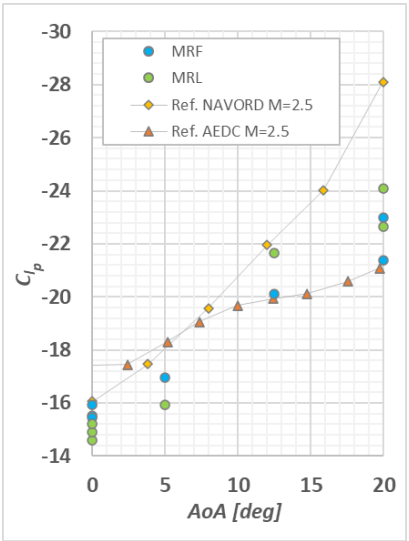

Figure 63 Variation of C_{lp} with incidence at Mach 2.5

The data presented are obtained by both MRF and MRL and show close values, consistent with the reference ones, except for the incidence of 20° where the obtained results seem to underestimate the reference data.

4.6. REMARKS

In the experimental study, two effective methods (MRF and MRL) for obtaining the damping coefficient on the roll axis were presented, as well as two methods for correcting the acquired data. The results obtained with the presented methods were compared with reference data from the specialized literature and the high degree of accuracy of the obtained data was shown. Furthermore, this study validated the proposed methodology for identifying the damping coefficient on the roll axis using the consumed power of the electric motor.

Both the forced rotation method (MRF) and the free rotation method (MRL) have both advantages and disadvantages. MRF although has better accuracy than MRL, requires a more complex acquisition system and longer acquisition times, while MRL has the advantage of short acquisition time and a simplistic acquisition system, but the data accuracy is poorer than MRF, and the raw data has oscillations, being a method with high sensitivity.

The tare correction is a very necessary first correction that can be applied in a very simple way, without the need for blowing tests. The determination of strength is optimally performed under vacuum conditions, but for convenience it can also be determined under atmospheric conditions. This correction avoids overestimation of the damping coefficient due to frictional effects in the clamping system, in the present case, from the bearings. Also in the tare correction category is the aerodynamic tare correction, this referring to the effects of friction in the bearings due to the aerodynamic loads acting on the model during the gust. This type of correction is very difficult to achieve, being more indicated to avoid it by using very high speeds of the model, so that the effect of the aerodynamic loads is negligible compared to the rolling moment.

The correction with the geometric deviation is also a very important correction, but it presents a high cost of realization as blowing tests with the model rotated in the opposite direction are required. A simplistic variant of applying the correction with the geometric deviation is the use of the straight line of variation of the rolling moment with the speed.

The experimental data obtained are consistent with the reference data both for variation with Mach number and variation with speed and angle of attack. The presence of small differences in the variation of the damping coefficient with the speed at low speeds is due to the effect of the aerodynamic force which becomes comparable to the damping moment. In the case of the variation of the damping coefficient with the angle of attack, small differences appear at higher incidences, the reason being also due to the aerodynamic force, which increases with the incidence due to the increase of the normal force on the model.

As a general conclusion of this chapter, it can be stated that the experimental study achieved its objectives, the device being developed, and the proposed identification and correction methodologies being tested and validated.

5. NUMERICAL STUDY

5.1. THE OBJECTIVES OF THE NUMERICAL STUDY

The numerical study presents the following objectives:

- Aerodynamic characterization in terms of roll axis aerodynamic damping coefficient for the Basic Finner standard model at various Mach numbers and angles of attack with the aim of extending the current databases and increasing their confidence;
- Identify the characteristics of the quasi-steady solution compared to the unsteady solution;
- Presentation of the variation of roll axis aerodynamic damping coefficient with roll angle for different Mach numbers and incidence angles;
- Presentation of the aerodynamic phenomena that occur during model rotation, presentation of the distribution of pressure coefficient and Mach number;

5.2. PRESENTATION OF SETTINGS CONSIDERED

5.2.1. Presentation of the calculation domain

The calculation domain used consists of two subdomains as shown in Figure 64. The first domain is the outer one, it has a spherical shape and a very large volume, having a diameter of D=100m. The second domain is the inner one, it has a cylindrical shape and a much smaller volume compared to the outer domain, having the diameter d=0.2m and the length L=0.75m so that it includes the analyzed model Basic Finner Model.

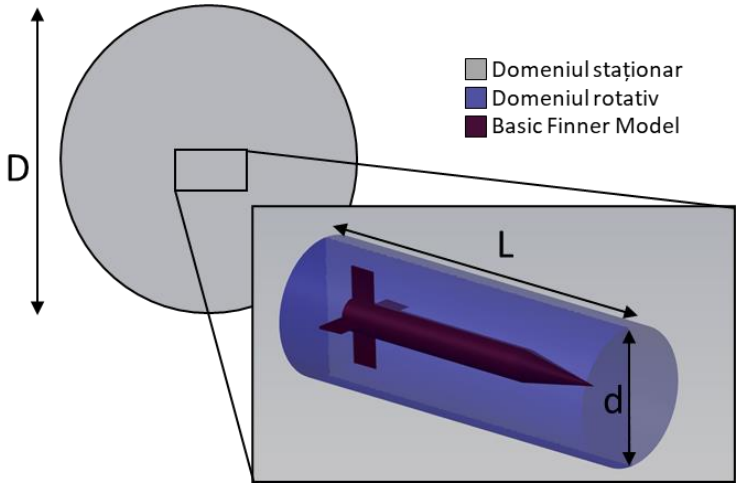

Figure 64 The calculation domain

5.2.2. Generation of the calculation grid

The computational grid used presents a hybrid structure between prismatic discretization (in the vicinity of the model) and polyhedral discretization (in the inner and outer domains). This approach allows for good geometry accuracy and a reduced number of cells.

Figure 65 shows the discretization of the model surface with details on the discretization on narrow regions such as the tip of the model and fins. It is observed that the discretization with hexagonal cells on the surface approximates the model very well even in the narrow regions, with small cells being used. Figure 66 shows the variation of the cells in the plane of symmetry for both the stationary domain and the rotating domain.

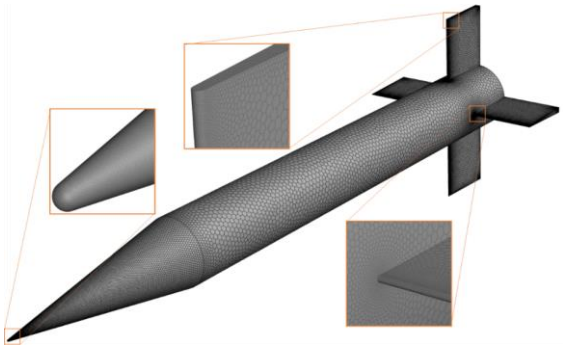

Figure 65 Discretization on the model surface

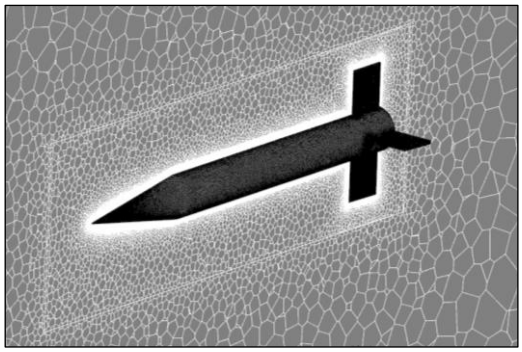

Figure 66 Discretization in the vertical plane

5.2.3. Setting the boundary conditions

In order to obtain high accuracy results, the following boundary conditions were imposed on the borders of the two domains. The outer boundary of the stationary domain presents *the pressure far-field* condition. The inner boundary of the stationary domain and its counterpart, the outer boundary of the rotating domain, present the *interface* condition. The inner boundary of the rotating domain, which also represents the surface of the model, exhibits the *no-slip wall* condition. .

5.2.4. Setting the solution model

The computational model solution method is implicitly using the Roe-FDS (Flux-Difference Splitting) scheme which exhibits accuracy and robustness for a wide range of applications. Solving the flow model is done in density, being a convenient option. Calculation of fluxes, turbulent kinetic energy and turbulent dissipation rate is performed with the 2nd order upwind scheme.

The characteristic time (L_{ref}/V_{∞}), where L_{ref} is the span of the model (0.18m), varies between 0.001317 for Mach = 0.4 and 0.000275 for Mach = 3.5. Thus, considering the dimensionless time (real time step / characteristic time) equal to 0.17453, the time steps for the analyzed cases are obtained.

5.3. PRESENTATION OF NUMERICAL ANALYSIS

5.3.1. The analysis matrix

The numerical analysis cases performed to determine the aerodynamic damping coefficients on the roll axis comprise five representative Mach numbers for the subsonic (Mach 0.4), transonic (Mach 0.95) and supersonic (Mach 1.6, 2.5 and 3.5) regimes. Six incidences were considered for each Mach number for a broad characterization of the damping coefficient as a function of Mach number and incidence. The angles of attack considered are: 0°, 10°, 20°, 30°, 40° and 50°.

5.4. THE RESULTS OBTAINED IN QUASI-STEADY REGIME

The numerical analyzes in the quasi-steady regime were carried out in order to present the precision of the results compared to the results obtained in the unsteady regime. The analyzes are carried out only for two regimes: Mach 0.4 and Mach 2.5, at incidences of 0°, 10° and 20°. Numerical simulations in unsteady regime are performed for roll angles between 0° and 90°, while numerical simulations in quasi-steady regime are performed at roll angles of 0°, 15°, 30°, 45°, 60°, 75° and 90°. The comparison between the solutioning methods are presented below:

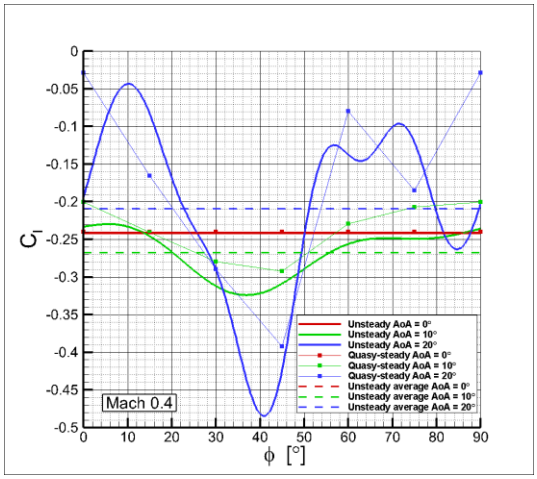

Figure 76 Cl vs ϕ at Mach = 0.4

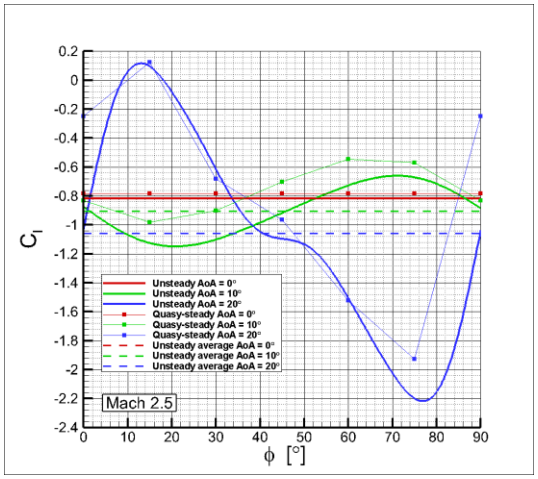

Figure 77 Cl vs ϕ at Mach = 2.5

5.5. THE RESULTS OBTAINED IN UNSTEADY REGIME

5.5.1. **Variation of C_{lp} with incidence and Mach number**

The variation of the damping coefficient on the roll axis with the angle of incidence and Mach number is presented in Figure 78 and Figure 79.

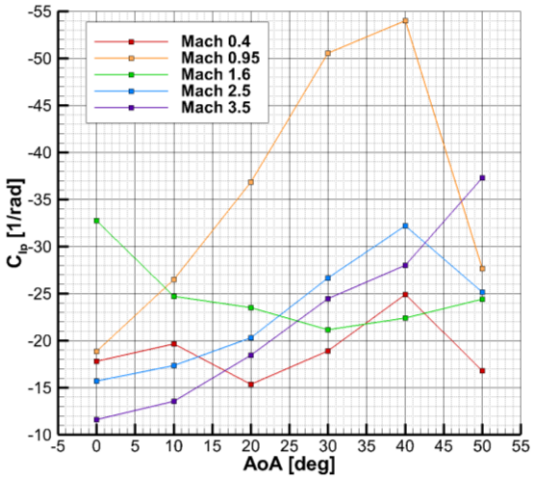

Figure 78 C_{lp} vs AoA

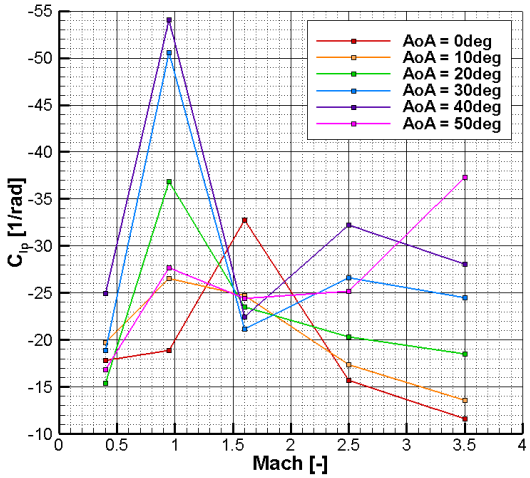

Figure 79 C_{lp} vs Mach

The fact that the presented variations are not typical and do not show a certain trend of variation is due to the derivative character of the damping coefficient and the aerodynamic interference phenomena present in the flow.

5.5.2. Variation of C_{lp} with roll angle

The figures below show the variation of roll axis damping coefficient with roll angle for different Mach numbers and incidence angles.

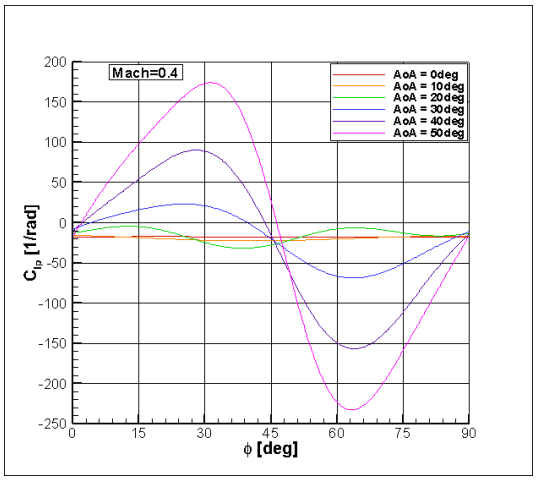

Figure 80 C_{lp} vs roll angle at Mach 0.4

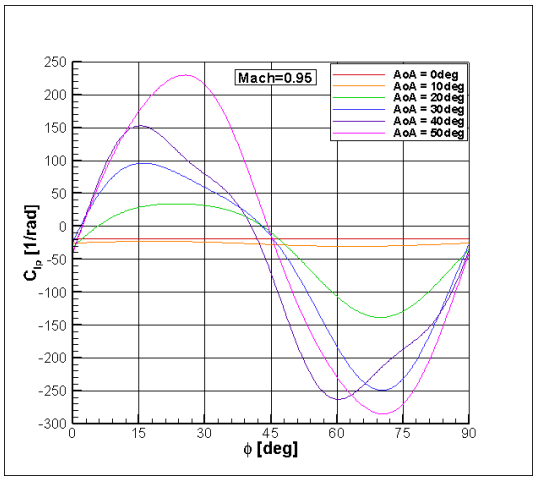

Figure 81 C_{lp} vs roll angle at Mach 0.95

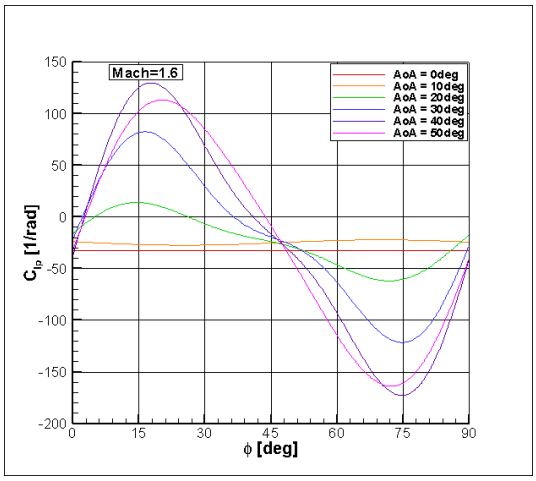

Figure 82 C_{lp} vs roll angle at Mach 1.6

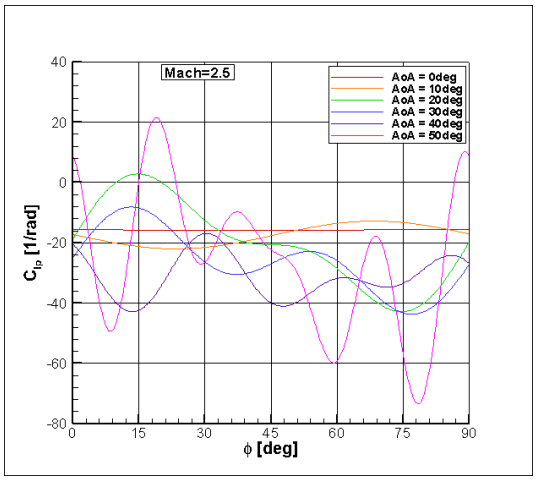

Figure 83 C_{lp} vs roll angle at Mach 2.5

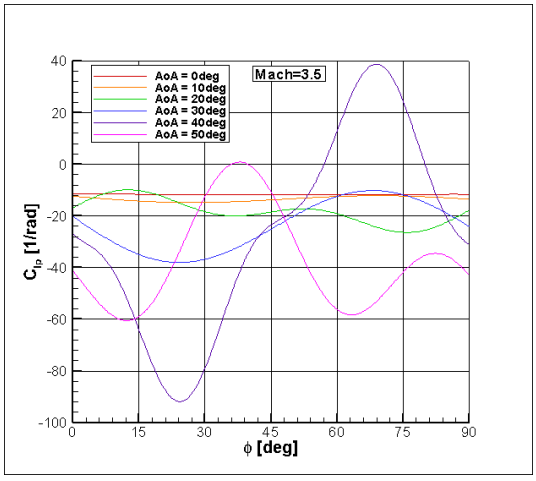

Figure 84 C_{lp} vs roll angle at Mach 3.5

5.6. GRAPHICAL ANALYSIS OF THE RESULTS

5.6.1. Cp and Mach distribution for different incidences

5.6.1.6. Remarks

The Cp distributions present the flow aspects in the vicinity of the model at the 0° roll angle position at the incidences of 0°, 10°, 20°, 30°, 40° and 50° for Mach numbers 0.4, 0.95, 1.6, 2.5 and 3.5, with the aim of understanding the variation tendency of the aerodynamic coefficients with both incidence angle and Mach number.

At zero incidence, the wings of the model experience the same incidence, the pressure distribution on their faces being identical between the four, thus resulting in zero aerodynamic coefficients except for the rolling moment coefficient. This aspect changes when the incidence increases due to the fact that the effective incidence on the fins varies with the roll angle thus generating a periodic variation of the aerodynamic coefficients. The period of variation of the aerodynamic coefficients is 90°, equal to the angular spacing between the fins.

Dorsally located wings show low pressure values due to the fact that they interact with the separation of the flow from the surface of the fuselage, and ventrally located wings show increased pressure values due to the fact that they are located in an free stream flow, and may even show stagnation zones

In the supersonic regimes the presence of interactions between the fins of the model and the ventral shock wave generated by the body of the model can be observed. This interaction induces sudden pressure variations on the wing which implies sudden variations in aerodynamic coefficients with roll angle.

5.6.2. Cp distribution for different roll angles

5.6.2.7. Remarks

The distribution of the pressure coefficient on the surface of the model at different roll angles and incidences, at Mach number = 2.5 is presented to exemplify the interactions that appear in the rotation of the model. This case was considered for exemplification due to the fact that it presents the strongest variations of the rolling moment coefficient with the roll angle, the phenomena present are complex and it is representative of this study.

The interaction between the dorsal flow and the fins consists in the loss of efficiency of the fins positioned downstream of the dorsal flow due to the wake generated by the flow separation. This interaction induces a pressure drop on the dorsal fins which causes a variation in the rolling moment.

The interaction between the ventral shock wave, generated by the body of the model, and the fins consists in the partial loss of the efficiency of the fins positioned on the ventral side of the body. At high incidences, the shock wave approaches the body of the model generating pressure variations on the ventral fins.

5.7. REMARKS

The numerical study presents the variation of the damping coefficient on the roll axis, C_{lp}, with Mach number (0.4, 0.95, 1.6, 2.5 and 3.5), angle of attack (0°,10°,20°,30°,40°,50°) and roll angle (0° - 90°). This study represents the most elaborate numerical study on the Basic Finner Model in rotation around the roll axis, thus continuing the numerical analyzes in papers [10], [8] and [6].

The obtained results show three variations of C_{lp}, namely: variation of C_{lp} with Mach number, variation of C_{lp} with incidence and variation of C_{lp} with roll angle. In addition to these variations, the distributions of Cp on the surface of the model and the distribution of the Mach number in the plane of symmetry for different incidences and Mach numbers (roll angle of 0°) and respectively the distribution of Cp on the surface of the model for different roll angles and angles of attack (Mach =2.5).

The variations of C_{lp} with incidence angle and Mach number showed that the trend of variation is strongly non-linear, which is due to the complex flow around a rotating model. The averaged values of the damping coefficient on the roll axis are strictly negative, which indicates a stability on the roll axis at all analyzed regimes.

The variations of C_{lp} with roll angle show the roll damping coefficient dependence on roll angle for different Mach numbers and incidence angles. These variations show that the dependence of C_{lp} on roll angle is a periodic function of period 90°, equal to the angular spacing between the fins. The variation of C_{lp} with the angle of incidence is constant as a result of the similar loading of the fins. Moreover, the amplitudes of the variations of C_{lp} with respect to the Mach number, at constant incidence, are constant in the subsonic and transonic regimes and decrease in the supersonic regimes. The supersonic regimes present additional oscillations compared to the subsonic and transonic regimes due to the interactions between the shock waves and the model.

The distribution of Cp and Mach shows at high incidences strong interactions of the fins of the model with the wake generated on the dorsal surface of the model and with the ventral shock wave generated by the body of the model, in the case of supersonic regimes. These interactions are correlated with Clp variations with roll angle, inducing sudden variations with large amplitudes at increased incidences and especially in supersonic regimes.

The distribution of Cp on the surface of the model at different roll angles and incidences, indicates a loss of efficiency of the dorsal fin, due to the positioning in the wake of the flow. A partial loss of effectiveness of the ventral wing also occurs at high incidences in supersonic regimes when it interacts with the ventral shock wave. Near the roll angle of 45°, the wings are similarly loaded two by two, the Clp amplitude relative to the mean being zero.

Therefore, the numerical study provides a database of roll damping coefficients for different Mach numbers, incidences and roll angles, presents the physics of the flow around the rotating model, and provides a comparative analysis between the quasi-steady and unsteady solution.

6. CONCLUSIONS AND OWN CONTRIBUTIONS

6.1. OBTAINED RESULTS

In conclusion, the paper presents experimental and numerical studies on the aerodynamic damping on the roll axis of the Basic Finner standard model, providing original contributions regarding the experimental identification methods of aerodynamic damping, experimental data correction methods, aerodynamic damping identification device that includes both the free rotation method and the forced rotation method, the extension of the experimental and numerical databases, a comparative numerical study between the quasi-steady solution and the unsteady solution, and last but not least, the analysis of the aerodynamic phenomena for the Basic Finner Model in roll rotation at different numbers Mach, incidence angles and roll angles.

In the first chapter, the foundations of the work, the specific objectives and the implementation plan are presented, these being necessary to address the problem of identifying the aerodynamic damping coefficient on the roll axis.

The paper presents in sections 2.1. and 2.2. a brief history and current status of aerodynamic roll damping determination devices, devices that extend the capability of the wind tunnels to dynamic regime testing. In sections 2.3. and 2.4, the theoretical notions underlying the testing in dynamic mode and the mathematical models used to determine the damping moment coefficient on the roll axis, both by the free rotation method and by the forced rotation method, are presented.

In the third chapter, the following sections are presented: 3.1. where the test model and the test matrix are specified; 3.2 where the experimental installation, namely the INCAS trisonic blower and the considered experimental techniques are presented, and respectively 3.3. where the considered calculation model and solution techniques are presented.

Chapter 4 presents: the specific objectives of the experimental study, the design of the test system, the experimentation campaign, the data processing programs, the results obtained and discussions on their account.

Section 4.1. presents that the main objectives of the experimental study are: aerodynamic characterization of the BFM, validation of the proposed MRF identification method, validation of the proposed geometric deviation correction method and the development of a device that uses MRF and MRL to identify the aerodynamic damping moment.

In section 4.2. the design and operation of the RDR device, its components, load estimation and mechanical strength analyzes performed by finite element analysis are presented in detail.

In the section 4.3. test characteristics, tare identification of the RDR system, BFM model deviations and the detailed experimental test matrix are presented.

Section 4.4. presents the calculation algorithm for determining the aerodynamic damping coefficients on the roll axis using the intensity of the current consumed through MRF and the variation of speed over time through MRL. The recorded values

are transformed into damping moments, and then into aerodynamic coefficients taking into account the flow parameters.

The obtained results are presented in section 4.5., where are analyzed: the influences of the tare corrections and with the geometric deviation of the model, the variation of speed with time, the variation of the damping moment with speed, the variation of C_{lp} with Mach number and the variation of C_{lp} with incidence. These analyzes are presented in comparison with reference data obtained in several experimental facilities by different methods.

In section 4.6. the observations are presented regarding: the accuracy of the results obtained compared to the reference results, the model for obtaining the results by the two methods and the aerodynamic phenomena that alter the obtained results. The general conclusions on the experimental study are that the specific objectives were fully met successfully, the results obtained present a very good accuracy for most cases excepting the tests at increased incidences or at reduced speeds where the influence of aerodynamic tare becomes considerable altering the data.

In chapter 5. 5. the following are presented: the specific objectives, the settings of the aerodynamic solution, the characteristics of the numerical analyses, the results obtained considering the quasi-steady and unsteady solution and the discussions related to the results obtained.

Section 5.1. presents the specific objectives of the numerical study consisting of: aerodynamic characterization of the BFM, comparative study between quasi-steady and unsteady solutions, presentation of the variation of C_{lp} with the flow parameters and specific aerodynamic phenomena.

Section 5.2. presents: the computational domain considered and its discretization, the boundary conditions imposed and the settings applied to the solution model. The computational domain is composed of two subdomains, one rotating and one stationary, which allows the use of both MRFT and SMT, the computational grid consists of polyhedral cells, resulting in a grid convergence study of about 9 million cells. The boundary conditions are: no-slip wall on the surface of the model, interface on the surface between the two domains and constant pressure on the surface outside the stationary domain. The solution model settings consist of: using the conservative model formulation and using the 2nd order up-wind Roe FDS scheme.

In section 5.3. the detailed numerical analysis matrix, the post-processing program of the obtained data and the validation of the numerical results with reference experimental data are presented. Validation of the results is performed for 0° incidence on the Mach range

Section 5.4. presents a comparative analysis between the quasi-steady and unsteady solutions. This analysis shows the advantages of a fast solution using MRFT with decent accuracy in results, but also the advantages of a solution with high accuracy in results using SMT. This study shows that MRFT can also be applied when the flow is not axial on the rotor, the results obtained being close to the results obtained in unsteady solution.

Section 5.5. shows the variation of C_{lp} with Mach number, with incidence and with roll angle. The obtained results show a strong non-linear character for the

variations with the incidence and the Mach number, and for the variations with the roll angle they show periodic variations with a period of 90° equal to the angular spacing between the fins of the model. It was observed that the variations with Mach number and angle of incidence do not show a characteristic trend. This fact is due to the complex effects present in the flow, highlighted in section 5.6. in the Cp and Mach distributions for different Mach numbers, incidences, and roll angles. The main interactions observed are between the dorsal wake and the fins, the ventral shock wave generated by the model body and fins, and the shock waves generated by the fins and the model body. These interactions create strong variations with the roll angle of the pressure distribution, which implies a strong non-linear character of the variation of the rolling moment with different flow parameters.

Section 5.7. presents the main observations on the obtained numerical results. This section summarizes the entire chapter, presenting the achievement of specific objectives and analyzing the aerodynamic effects in the flow field.

Therefore, the obtained experimental and numerical results present a very good accuracy, contributing to the characterization of the aerodynamic damping moment on the roll axis of the Basic Finner Model. The experimental results obtained by MRL and MRF allowed the validation of the proposed identification method and also increased the confidence of the reference data.

The realized RDR device presents a simplistic way of identifying the damping moment on the roll axis during a wind tunnel run by two independent methods. This device is unique in having the following characteristics: it uses the MRF and MRL methods, it measures the roll axis damping moment using the motor power consumption, and it is a compact system with an aerodynamic shape for minimum interactions with the model.

The numerical results obtained are validated with experimental reference data for certain regimes, thus making it possible to characterize the model in terms of the damping coefficient on the roll axis for a wide range of Mach numbers, incidence angles and roll angles. The presented aerodynamic phenomena explain the strongly non-linear variations of the dependence of C_{lp} on the flow parameters.

6.2. ORIGINAL CONTRIBUTIONS

The original contributions made in the work are as follows:

- Method of identifying the damping coefficient on the roll axis using the forced rotation method. This method is presented in the sections *2.4.1.* and *3.2.2.1.* , but also in the paper [19].
- Method for correcting the roll moment coefficient with the geometric deviation. This method is presented in the sections *2.4.1.* and *4.5.1.2.* but also in the paper [19].
- Experimental database at various Mach numbers, angles of attack and rotation speeds for the Basic Finner calibration model. These data are presented in the sections *4.5.3.* , *4.5.4.* and *4.5.5.* , but also in the papers [19] și [48].
- Aerodynamic damping identification device on the roll axis that uses both the free rotation method and the forced rotation method. This device is presented in the section *4.2.* as well as within the patent application no. a 2023 00295, available in Figure 151.
- Study on the accuracy of the results obtained by the quasi-steady solution versus the unsteady solution in aerodynamic damping identification problems. This analysis is presented in the section *5.4.* and also in the paper [49].
- Extensive roll damping coefficient database for the Basic Finner Model at various Mach numbers, incidence angles and roll angles. This database is presented in the section *5.5.* and in the paper [33]
- Analysis of aerodynamic phenomena at different regimes presented in the sections *5.6.* and *5.7.* , but also in the paper [33]
- Publication of five scientific papers.
- Application for patenting the RDR device.

The above-mentioned represent original contributions of the author on the identification of the aerodynamic damping coefficient on the roll axis both experimentally and numerically.

6.3. LIST OF PAPERS AND PRESENTATIONS

6.3.1. List of scientific papers

During doctoral studies, the author published five scientific papers related to the subject of this paper as follows:

1. **Ionuț Bunescu**, Mihai-Vlăduţ Hothazie, Mihai-Victor Pricop and Mihăiţă Gilbert Stoican, *Roll Damping Measurements on Basic Finner Model Using Both Forced and Free Methods*, Journal of Spacecraft and Rockets, Vol. 60, Issue 6, 2023.
2. **Ionut Bunescu**, Stefan Bogos, Teodor-Viorel Chelaru, Mihai-Vladut Hothazie, Mihai-Victor Pricop, *Coherent solutions to roll damping derivatives evaluation for a generic rocket model*, INCAS BULLETIN, Vol.15, Issue 3,pp. 19-30, 2023.
3. **Ionuț Bunescu**, Mihai-Victor Pricop, Mihăiță-Gilbert Stoican, Mihai-Vlăduț Hothazie, *Identification of roll damping coefficient using the free rotation method*, INCAS BULLETIN, in press.
4. **Ionuț Bunescu**, Teodor Viorel Chelaru, Mihai-Victor Pricop, Mihăiță Gilbert Stoican, Mihai-Vlăduț Hothazie, *Experimental Studies of Roll Damping Coefficient for Basic Finner Model*, AIP, in press.
5. **Ionuț Bunescu**, Mihai-Vlăduț HOTHAZIE, Tudorel-Petronel AFILIPOAE , Alexandru-Iulian ONEL, Mihai-Victor PRICOP, *A Comparison of Quasi-Steady and Unsteady CFD Methods on Roll Damping Derivatives Evaluation*, AIP, in press.

Among them, paper 1 is published in a WoS indexed journal (Impact factor 2022: 1.6, Q3), papers 4 and 5 are published in WoS indexed journals, and papers 2 and 3 are published in the INCAS Bulletin journal indexed in the BDI.

6.3.2. List of technical and scientific presentations

During doctoral studies, the author presented nine papers at international scientific events and participated in three presentations at international technical-scientific events. These are set out in the following:

1. **Ionuț Bunescu**, Mihai-Victor Pricop, Mihăiță-Gilbert Stoican, Ruxandra Dușmănescu, *Development of damping rigs for trisonic wind tunnel*, International Conference of Aerospace Sciences, Bucharest, October 2020.
2. **Ionuț Bunescu**, Mihai-Vlăduț Hothazie, Mihai-Victor Pricop, Mihăiță-Gilbert Stoican, *Roll damping coefficient determination and correction for Basic Finner Model*, International Conference of Aerospace Sciences, Bucharest, October 2022.
3. Mihai-Vladut Hothazie, **Ionuț Bunescu**, Mihai-Victor Pricop, Dumitru Pepelea, *CFD Numerical Predictions for Aerodynamic Roll Damping Coefficients on Basic Finner Model*, International Conference of Aerospace Sciences, Bucharest, October 2022.
4. Ciprian Chivu, **Ionuț Bunescu**, *Roll Damping Rig – Design and Validation*, STAI 134th Meeting 2022, Bedfort, October 2022.

5. **Ionuț Bunescu**, Mihai-Vladut Hothazie, Mihai-Victor Pricop and Mihăită-Gilbert Stoican, *Roll Damping Measurements on Basic Finner Using Both Forced and Free Methods*, AIAA SciTech Forum, National Harbor & Online, January 2023.
6. **Ionuț Bunescu**, Mihai-Victor Pricop, Mihai-Vlăduț Hothazie, Mihăiță-Gilbert Stoican, *Experimental investigation on roll damping coefficient*, 9thInternational Workshop on Numerical Modelling in Aerospace Sciences, Bucharest, May 2023.
7. **Ionuț Bunescu**,Mihai-Vlăduț Hothazie, Ciprian Chivu, Mihai-Victor Pricop, Mihăiță-Gilbert Stoican, Nae Cătălin, *Roll Damping Rig validation with Basic Finner Model in dual mode: forced and free rotation method*, STAI 135th Meeting 2023, Tel Aviv, May 2023.
8. **Ionuț Bunescu**, Teodor Viorel Chelaru, Mihai-Victor Pricop, Mihăiță-Gilbert Stoican, Mihai-Vlăduț Hothazie, *Experimental Studies of Roll Damping Coefficient for Basic Finner Model*, International Conference for Nonlinear Problems Aeronautics and Aerospace, Praga & Online, June 2023.
9. **Ionuț Bunescu**, Ștefan Bogos, Teodor-Viorel Chelaru, Mihai-Vladut Hothazie, Mihai-Victor Pricop, Coherent solutions to roll damping derivatives evaluationfor a generic rocket model, EUCASS & CEAS, Laussane, July 2023.
10. **Ionuț Bunescu**, Mihai-Vlăduț HOTHAZIE, Tudorel-Petronel AFILIPOAE , Alexandru-Iulian ONEL, Mihai-Victor PRICOP, *A Comparison of Quasi-Steady and Unsteady CFD Methods on Roll Damping Derivatives Evaluation*, International Conference of Numerical Analysis and Applied Mathematics, Heraklion, September 2023..
11. **Ionuț Bunescu**, Ștefan Bogos, Teodor-Viorel Chelaru, Mihai-Vlăduț Hothazie, Mihai-Victor Pricop, Mihăiță-Gilbert Stoican, *Evaluation methods for roll damping coefficient*, The 40th "Caius Iacob" Conference on Fluid Mechanics and its Technical Applications, Bucharest, October 2023.
12. **Ionuț Bunescu**, Mihai-Vladut Hothazie, Mihai-Victor Pricop, Alexandru Onel and Tudorel Afilipoae, *Numerical Investigation of Basic Finner Model in Roll Motion as Complement to the Experimental Work*, AIAA SciTech Forum, Orlando, January 2024.

6.3.3. List of patents and industrial designs

The author, together with the collaborators, proposed a patent application to OSIM in order to patent the device used in the experimental study. It presents the following details:

1. **Ionuț Bunescu**, Ciprian Chivu, Mihai-Victor Pricop, Mihai-Vlăduț Hothazie, Dispozitiv de identificare a amortizării aerodinamice pe axa de ruliu, Request no.: a 2023 00295, 2023.

6.4. PROSPECTS FOR FUTURE DEVELOPMENT

The paper presents two broad perspectives for further development:

The first perspective is to integrate a strain gauge on the axis of the device so that all aerodynamic forces and moments developed during rotation can be determined. In addition to the aerodynamic damping on the roll axis and the derivatives of the lateral force and the yaw moment with reduced rotation around the roll axis, aerodynamic coefficients of interest called the Magnus moment coefficient and the Magnus force coefficient can thus be obtained. This approach has the huge advantage of testing at very low angular speeds without the contribution of downforce. The challenge in this case is to integrate the balance within the device and protect it from aerodynamic stresses, also the connection of the balance is a challenge, requiring circular connecting brushes or other connections. A simplistic approach may be to rotate the model at low speeds over a narrow range of roll angles so that the balance wires are not pulled. This approach can be applied to vehicles with slow motion around the roll axis, such as aircraft.

The second perspective consists in the development of a similar device to determine the aerodynamic damping around the pitch and yaw axes. Such a device is of great interest due to the importance of the damping coefficients on the pitch and yaw axes (C_{mq} and C_{nr}), these coefficients being difficult to estimate by numerical simulations. Its use for pitch and yaw damping can be achieved by simply rotating the device 90°. Similar to the roll axis aerodynamic damping identifier, a pitch and yaw axis damping identifier can use either the free oscillation method or the forced oscillation method. The free oscillation method consists of a system for removing the model from equilibrium and an elastic system that induces an oscillatory movement of the model around an equilibrium position, the determination of the damping coefficient on the pitch/yaw axis being carried out by using the logarithmic decrement relation. The forced oscillation method consists of a system for moving the model at constant angular speed and a system for measuring the pitch/yaw moment during movement around the pitch/yaw axis, the damping coefficient being obtained by dividing the measured moment coefficient by frequency of oscillation. The challenges of developing such a device are: accurately measuring the oscillation of the model avoiding the secondary modes given by the clamping of the model and the device, positioning the model at the desired angle, achieving frequency similitudes and moment of inertia similitudes, in addition to the similitudes in Mach number and. Reynolds number.

A device for identification of aerodynamic damping on the pitch/yaw axis is being developed and tested under the HiSAEROD project (671 PED) which also funded the development and testing of the RDR system presented in this paper.

7. BIBLIOGRAPHY

[1] C. Schueler, L. Ward și A. Hodapp, „Techniques for measurement of dynamic stability derivatives in ground test facilities," Advisory group for aerospace research and development, 1967.

[3] M. Samardzic, J. Isakovic, M. Milos, Z. Anastasijevic și D. B. Nauparac, „Measurement of the Direct Damping Derivative in Roll of the Two Callibration Missile Models," *FME Transactions,* vol. 41, nr. 3, pp. 189-194, 2013.

[8] V. A. Bhagwandin, „High-Alpha Prediction of Roll Damping and Magnus Stability Coefficients for Finned Projectiles," *Journal of Spacecraft and Rockets,* vol. 53, nr. 4, pp. 720-729, 2016.

[10] M. R. Eidell, R. P. Nance, G. Z. McGowan, J. G. Carpenter și F. G. Moore, „Computational Investigation of Roll Damping for Missile Configurations," în *30th AIAA Applied Aerodynamics Conference*, Louisiana, 2012.

[14] J. Nicolaides și R. Bolz, „On the Pure Rolling Motion of Winged and/or Finned Missiles in Varying Supersonic Flight," *Journal of the Aeronautical Sciences,* vol. 8, pp. 160-1683, 1953.

[15] F. Regan, „Roll Damping Moment Measurement for the Basic Finner at Subsonic and Supersonic Speeds," NAVORD, 1964.

[16] B. Uselton și L. Jenke, „Experimental Missile Pitch- and Roll-Damping Characteristics at Large Angles of Attack," *Journal of Spacecraft and Rockets,* vol. 14, pp. 241-247, 1977.

[17] S. M. Murthy, „Subsonic and Transonic Roll Damping Measurement on Basic Finner," *Journal of Spacecraft and Rockets,* vol. 19, nr. 1, pp. 86-87, 1982.

[19] I. Bunescu, M.-V. Hothazie, M.-V. Pricop și M. G. Stoican, „Roll Damping Measurements on Basic Finner Using Both Forced and Free Methods," în *AIAA Scitech 2023 Forum*, National Harbor, 2023.

[29] L. Jenke, „Experimental Roll-Damping, Magnus and Static-Stability Characteristics of Two Slender Missile Configuration at High Angles of Attack (0 to 90 deg) and Mach Numbers 0.2 through 2.5," Arnold Engineering Development Center, 1976.

[30] S. Murthy, P. Rao și N. Vasudeva, „Development of a roll-damping test rig for measurements on continuously rotating models in the NAL 0.3m Trisonic Blowdown Tunnel," NAL Report: AE-TM-1-81, 1981.

[33] I. Bunescu, M.-V. Hothazie, M.-V. Pricop, A. Onel și T. Afilipoae, „Numerical Investigation of Basic Finner Model in Roll Motion as Complement to the Experimental Work," în *AIAA SCITECH 2024 Forum*, Orlando, 2024.

[48] I. Bunescu, T. Chelaru, M. Pricop, M. Stoican și M. Hothazie, „Experimental Studies of Roll Damping Coefficient for Basic Finner Model," *AIP,* in press.